Graphical Abstract (for review)

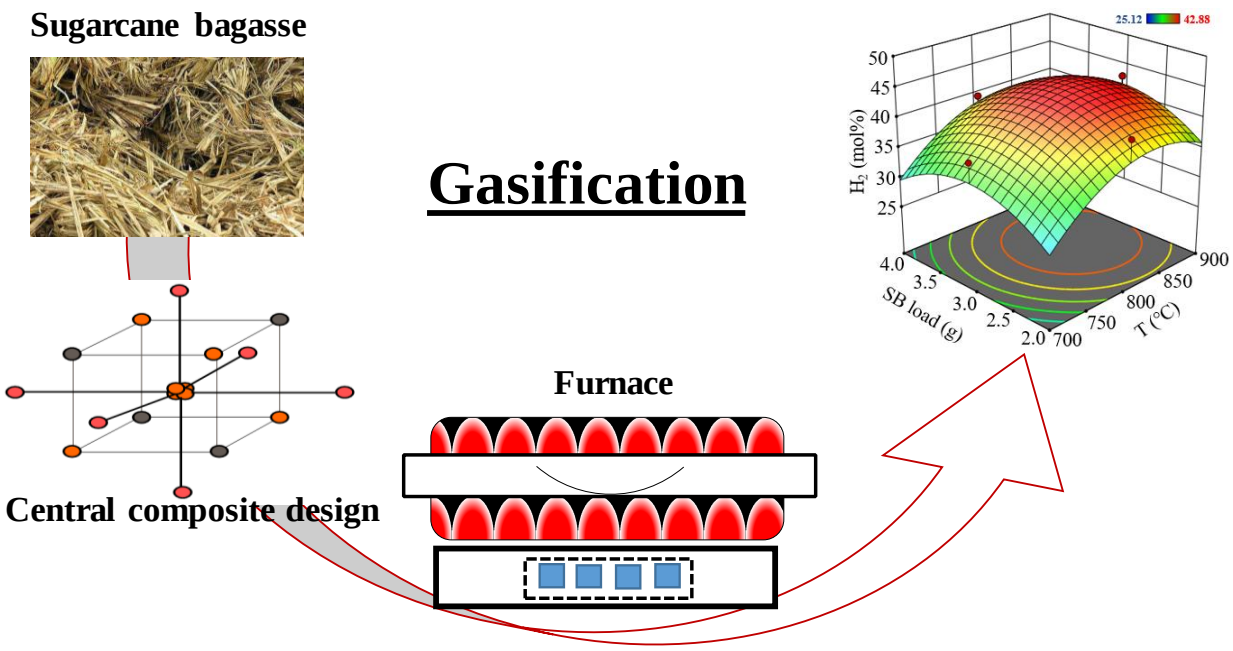

Highlights

- Conventional gasification of sugarcane bagasse was investigated.
- Central composite design was adopted to determine the parametric effect on syngas.
- Higher temperatures and reaction time favored H_2 yield and reduction of tar and char.
- H_2 fraction peaked at 36.91 g-H_2 kg-biomass^{-1} at 3g of SB loading, 900℃ for 30min.

Parametric gasification process of sugarcane bagasse for syngas production

Abdul Raheem,[1] Ming Zhao,[1] Wafa Dastyar,[1] Abdul Qadir Channa,[2] Guozhao Ji,[3] Yeshui Zhang[4]*

[1.] School of Environment, Tsinghua University, Beijing 100084, China

[2.] Mechanical Engineering Department, Quaid-e-Awam University of Engineering Science and Technology, Pakistan 67450.

[3.] School of Environmental Science & Technology, Dalian University of Technology, Dalian 116024, Liaoning, China

[4.] Electrochemical Innovation Lab (EIL), Department of Chemical Engineering, University College London, Torrington Place, London, WC1E 7JE.

* Corresponding Author: Tel: +86 10 62784701; Emails: ming.zhao@tsinghua.edu.cn

Abstract

This research focuses on parametric influence on product distribution and syngas production from conventional gasification. Three experimental parameters at three different levels of temperature (700, 800 and 900 °C), sugarcane bagasse loading (2, 3 and 4 g) and residence time (10, 20 and 30 min) were studied using horizontal axis tubular furnace. Response Surface Methodology supported by central composite design was adopted in order to investigate parameters impact on product distribution (i.e., gas, tar and char) and gaseous products (i.e., H_2, CO, CO_2 and CH_4). The highest H_2 fraction obtained was 42.88 mol% (36.91 g-H_2 kg-biomass^{-1}) at 3 g of sugarcane bagasse loading, 900 °C and 30 min reaction time. The temperature was identified as the most influential parameter followed by reaction time for H_2 production and diminishing the bio-tar and char yields. An increase in sugarcane bagasse loading, on other hand, favored the production of bio-tar, CO_2 and CH_4 production. The statistical analysis verified temperature as most significant (*p*-value 0.0008) amongst the parameters investigated for sugarcane bagasse biomass gasification.

Keywords: Sugarcane bagasse, Biomass gasification, parametric effect, hydrogen fuel, central composite design

1. Introduction

The importance of exploring renewable and sustainable energy options have become imperative, to improve energy security, especially due to limited fossil fuel reserves and current adverse climatic changes [1]. The alternative energy options and production systems must be considered based on availability, affordability and equity. Biomass is considered a low carbon substitute to fossil fuels, in particular for low greenhouse gas emissions (GHGs). Amongst the various biomasses, agricultural waste and process biomass are viable options. Nevertheless, biomass based energy production would enable the concurrent decrease of GHGs into environment [2]. It has been anticipated that future energy utilization will have increased dependence on varied energy mix, particularly resulting from biomass. Thus, opt advancement to utilize the biomass for energy generation will have a remarkably positive impact in sustaining future energy estimates. In comparison with the utilization of dedicated crops, the application of residues as biofuel feedstock instead of their disposal would result in lower net impact and emissions. This could counterbalance fossil fuel inputs in biofuel processing [3]. The exploitation of non-edible feedstock for biofuel production also prevents impediments associated to food supply [4], which are present in first-generation biofuels.

Sugarcane bagasse (SB) is the lignocellulosic fibrous leftover acquired after the sucrose-rich juice extraction. SB owns about 50 % of cellulose, 25 % of hemicellulose and 25 % of lignin [5]. In general, one ton of SC results approximately 100 kg of sugar, ~270 kg of dry bagasse and ~35 kg of molasses [6]. It is assessed that 540 million t/y of SB is generated worldwide, indicating considerable potential for commercial-scale biofuel production [7]. SB is mainly utilized in boiler for steam production; thereby generating electricity to power the sugar mills. However, the approach is challenged by lower electrical efficiency(20 %) against the

gasification process(80 %) [8, 9]. Recently, there has been increasing attention for an effective exploitation of agricultural wastes, comprising SB in an integrated industrial conversion units, [9] therefore entailing in an appropriate model of a true bio-refinery concept. Several conversion processes such as fermentation [10-13], anaerobic digestion [14-16], combustion [17-19], pyrolysis [20-22], supercritical water (SCW) gasification [5, 23, 24] have used SCB as a feedstock for development of sustainable energy systems and these include the bioethanol, methane, bio-oil and hydrogen, including other value added products [25].

Of all the conversion technologies, gasification has been considered as the most promising approach on the account of its advantages such as auto-thermal ability, high carbon conversion, higher calorific value (than the combustible gases derived from pyrolysis) of the syngas [1, 26]. Generally, gasification is a process based on five discrete fundamentals namely drying, pyrolysis, combustion, cracking and reduction. It converts biomass into synthetic gas (syngas) (H_2, CO, CO_2 CH_4 and other hydrocarbons) in the presence of oxygen or air at high temperature range (700 – 1000 ℃) [26, 27]. Syngas is a useful flammable gas which can be used to power the gas turbines and engines, boilers, and synthesis of various value added chemicals for instance methanol, gasoline e.g., through Fishcher-Tropsch. The sufficient availability of SB makes it suitable candidate as feedstock for gasification conversion. As a result, plenty of research papers have been published on supercritical water gasification of SB, mainly focusing on the parametric effect on H_2 production and gasification efficiency. For instance, Cao et al. gasified SB in SCW at temperature ranging from 600 – 750 ℃, SB loading 3 – 12 wt.% and residence time 5 – 20 min in the presence of Raney-Ni, K_2CO_3 and Na_2CO_3. H_2 yield peaked at 35.3 mol kg^{-1} at 650 ℃, SB loading 6 wt.%, residence time 15 min under Na_2CO_3 loading of 20 wt.% [5]. Tavasoli et al. performed

catalytic SCW gasification of SB in the presence of potassium (k) and copper (Cu). Results revealed noteworthy role of K to improve the H_2 selectivity from 0.76 to 1.17 [28]. Barati et al. scrutinized the effect on H_2 production from SB under un-promoted and zinc promoted Ru/g-Al_2O_3 nano-catalysts. The highest H_2 yield of 15.6 mol kg^{-1} was reported [29]. Similarly, another researcher investigated the effect of biomass loading, water density on SCW of SB in the presence of Ru/C and Ru/TiO2 catalyst. The complete gasification of SB into CH_4, CO_2 and H_2 over Ru/C and Ru/TiO_2 catalyst was achieved at 400 ℃[30].

However, on the basis of our knowledge, none of previous research has highlighted the conventional gasification (dry gasification) behavior of SB. Also, there has not been any systematic approach for the parametric optimization of the SB dry gasification towards higher H_2 production. The optimization and simulation of experimental parameters (such as temperature, biomass loading, reaction time, etc.) will help to achieve satisfactory levels of operating conditions towards the desired responses, where they will not be affected by variations in the factor setting. Therefore, it is crucial to optimize the operating conditions via a systematic experimental method such as response surface methodology (RSM) with the aid of central composite design (CCD). RSM-CCD is a scientific experimental design which has been effectively used for biomasses other than SB to optimize/observe the effect of multiple gasification experimental parameters on desired products and other associated multifactor findings [31, 32]. The major advantage of employing RSM-CCD is to acquire concise set of data and to determine the optimum conditions for required products with a low number of runs. Therefore, current study explores the SB conventional gasification for syngas production via RSM-CCD design. The multifactor parametric influence (i.e., temperature, SB loading, and residence time) on gaseous products, tar and char is studied in detail.

2. Materials and methods

2.1 Biomass and characterization

SB was obtained from a SC juice shop at Hyderabad Pakistan. The sample was sun dried from a week and chopped to reduce the particle size (PS). The PS was measured to be ~100 µm to 1 mm. The proximate analysis (i.e., such as moisture, volatile matter, fixed carbon and ash contents) of SB was performed by standard method as reported by Varma and Monal, 2016 [33]. The ultimate analysis such as carbon, hydrogen, nitrogen and sulfur contents of SB were evaluated via CHNS elemental analyzer (Elementar Vario EL III model). The oxygen content was evaluated by difference. The comparison of proximate and ultimate analysis of SB sample with earlier research work is presented in Table 1.

Table 1. Biomass characteristics

Biomass characterization	**Composition (wt %)**	**Doumer el al. [34]**	**Balasundram et al. [35]**
Proximate analysis			
Moisture	5.4±0.3	6.3	4.99±0.1
Volatile matter	81.3±0.2	83.03±0.67	73.50±0.99
Fixed carbon	10.2±0.4	12.97±0.58	19±0.17
Ash	3.1±0.3	4.00±0.18	2.34±0.8
Ultimate analysis			
C	45.98±0.8	45.52±0.22	44.32±0.51
H	6.2±0.3	6.26±0.01	6.04±0.46
N	0.4±0.2	0.24±0.03	0.53±0.02
S	0.07±0.01	0.00	0.24±0.03
O*	47.35±3.5	43.83±0.38	48.87±0.59
HHV** (MJ kg^{-1})	16±0.4	17.27±0.49	18.6±0.44

* $O = 100\% - C - H - N - S = O$

** $HHV = 33.86*C + 144.4*(H-O/8) + 9.428*S$ [36]

2.2. Experimental procedure

Fig. 1 details the reactor configuration used for the gasification of SB biomass experiments. The reaction tube has a diameter of 14 mm. The experimental setup mainly comprises of reactor, gas cleaning section (moisture trap containing silica gel) and clean gas collection via sampling bag and analysis. The study was conducted by investigating dissimilar experimental

parameters; temperature (700, 800 and 900 ℃), SB loading (2, 3 and 4 g) and residence time (10, 20 and 30 min). The experimental parameters were preset to facilitate smooth operation of reactor. During the experiment, the SB sample was placed in a quartz sampling boat and heated to desired temperature at constant heating rate of 10 ℃ min^{-1} for each run. Oxygen (5% O_2/Ar) with argon was introduced into reactor with the constant flow rate of 20 mL min^{-1}. After the temperature program started, gasifying agent was introduced into the reactor. The starting point of the temperature program was set to be 50 ºC. The produced gas was then passed through a gas cooling system filled of wool (this allows produced gas to be cooled down) followed by a moisture trap section filled with silica gel (to absorb the moisture). The sampling bag was used to collect the gas flowing out of moisture trap section. The gas sample was collected once the temperature of 100 ℃ was attained. A manual gas chromatography (GC) (model: 6890 Agilent) connected with two columns namely Varian capillary (HP-PLOT/Q) and molecular sieve (HP-MOLSIV) and a thermal conductivity detector was used for detailed analysis of the gaseous products. 0.25 mL of the gas sample was injected into the column at 60 ℃. Firstly, CO_2 was stripped in the HP-PLOT/Q followed by the fractionation of H_2, CO and CH_4 in the HP-MOLSIV through a synchronized dual valve injection system. In addition, tar and char were collected after the reactor was cooled down to atmospheric temperature. Tar contents were determined via weight difference of the reactor tube before and after each run. Similar approach was adopted for all runs. The reactor, tubing, gas cooling system and sampling bags were purged with nitrogen to eradicate trapped gas molecules prior to each run.

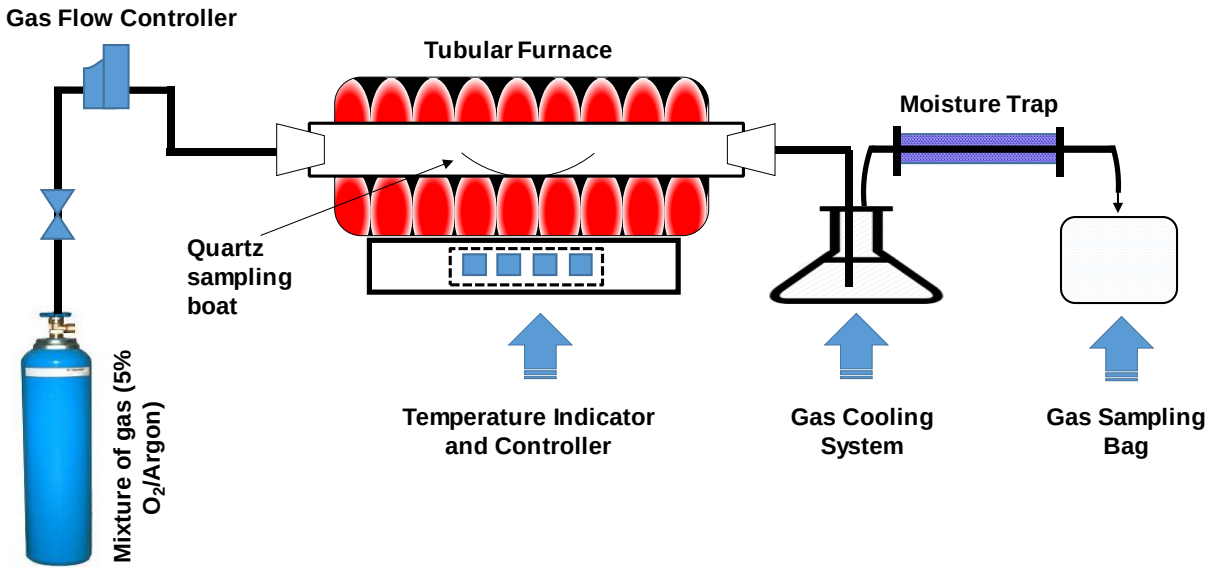

Fig. 1. Schematic diagram of experimental setup

2.3. Experimental approach

CCD is a scientific response surface methodology used study to determine the optimize levels of temperature, SB loading and residence time as independent variables for desired response variables. RSM-CCD method was used to design the experiments based on aforementioned operating parameters and four responses by using Design of Expert software (DX v. 10), while face centered mode (alpha = 1) was used which is without repeating the center point resulting in 15 different runs. The gas, bio-tar and char were dependent variables. Results were statically analyzed via the Statistica software (Statsoft, v.8.0). The influence of each parameter was identified to understand how the response of a combination of experimental parameters could results in the highest H_2 production. The experimental design and desired responses for SB gasification are shown in Table 2. The overall gas yield (wt.%) was determined by analyzing the char and tar products weight percent of the biomass loaded as indicated in eq (1). The initial biomass loading and final products (such as tar and char) were weighed using Apollo Precision Taploading Balance (Model: GX-4002a) with 4200 g maximum capacity and 0.01 g minimum readability. The lower heating value of gas was determined using eq (2) based on the species with combustion value [37].

$$Total\ gas\ (wt.\%) = 100\ wt.\ \% - tar\ (wt.\%) - char\ (wt.\%) \quad (1)$$

$$LHV\ (MJ\ N\ m^{-3}) = (H_2\ (vol\ \%) \times 107.98 + CO\ (vol\ \%) \times 126.36 + CH_4\ (vol\ \%) \times 358.18) /1000 \quad (2)$$

The same method for determination of total gas has been reported by other researches [38, 39].

Table 2. Experimental design matrix and results. The data presented is the average values of 2 repeats.

	Temp. (ºC)	SB load (g)	RT (min)	H_2 actual and predicted values (mol %)			H_2 (g kg-biomass^{-1})	Other response variables (mol %)			LHV MJ Nm^{-3}
				Actual	Predicted	Residual		CO	CO_2	CH_4	
1	700 (-1)	2 (-1)	10 (-1)	27.28	28.62	-1.34	16.30	19.80	33.95	18.97	12.24
2	700 (-1)	2 (-1)	30 (1)	28.48	28.61	-0.13	18.28	21.69	28.97	20.86	13.28
3	700 (-1)	3 (0)	20 (0)	37.57	35.96	1.60	28.19	23.83	22.86	15.74	12.70
4	700 (-1)	4 (1)	10 (-1)	25.12	25.07	0.04	14.64	20.24	34.97	19.67	12.31
5	700 (-1)	4 (1)	30 (1)	32.25	32.41	-0.16	21.96	23.12	27.21	17.42	12.64
6	800 (0)	2 (-1)	20 (0)	41.23	39.25	1.97	34.23	17.85	22.92	18.00	13.15
7	800 (0)	3 (0)	10 (-1)	41.12	39.51	1.60	33.48	16.37	23.63	18.88	13.27
8	800 (0)	3 (0)	20 (0)	41.59	44.02	-2.43	34.34	20.22	22.64	15.55	12.61
9	800 (0)	3 (0)	30 (1)	42.23	42.61	-0.38	36.01	20.43	20.98	16.36	13.00
10	800 (0)	4 (1)	20 (0)	39.42	40.17	-0.75	30.59	19.11	25.14	16.33	12.52
11	900 (1)	2 (-1)	10 (-1)	35.58	35.71	-0.13	25.56	18.86	30.12	15.44	11.75
12	900 (1)	2 (-1)	30 (1)	34.21	34.56	-0.35	26.12	20.54	25.37	19.88	13.41
13	900 (1)	3 (0)	20 (0)	42.88	43.26	-0.38	36.91	22.66	20.34	14.12	12.55
14	900 (1)	4 (1)	10 (-1)	33.57	33.73	-0.16	24.25	21.28	26.10	19.05	13.13
15	900 (1)	4 (1)	30 (1)	40.98	39.93	1.04	35.24	23.00	19.13	16.89	13.38

3. Results and Discussion

3.1 Analysis of product distribution

Fig. 2 shows the fractions of reaction products during the SB biomass gasification at different experimental conditions reported in Table 2. Typically, the gas is the major product produced during the gasification of biomass. Meanwhile, some amount of the biomass could be converted to the tar and char by-products of biomass gasification process. Generally, bio-tar is considered as an undesired by-product and it can result in many serious obstacles for instance blockage of gasifier due to condensation, development of tar aerosols and metal corrosion etc. Whilst, char is mainly resulted during the pyrolysis stage [40, 41]. As shown in Fig. 2, the gas was significantly higher than tar and char within experimental parameters range examined. Conversely, tar was found to be the second highest product, particularly at lower temperatures and shorter residence time. In current study, the obtained yields of gas, tar and char peaked from 71.91 to 79.33 wt.% (see run 1 and 12 in Fig. 2), 10.1 to 15.23 wt.% (see run 13 and 1 in Fig. 2), and 9.85 to 12.86 wt.% (see run 12 and 1 in Fig. 2), respectively, which indicates that gasification of SB own a great potential for gaseous production.

Fig. 3 (a – f) shows the combine effect of experimental parameters (i.e. temperature, SB loading and residence time) on composition of products (gas, tar and char) from the gasification of SB biomass. It can be observed from the experimental results (Fig. 3 a – f) that gasification product distribution was considerably influenced by the reactor temperature followed by residence time. According to Fig. 3 a and b, the increased reactor temperature and residence time promote the

increased production of gas mainly from conversion of bio-tar (Fig. 3 c and d), whereas minimal impact of SB on gas production could be seen (Fig. 3 a).

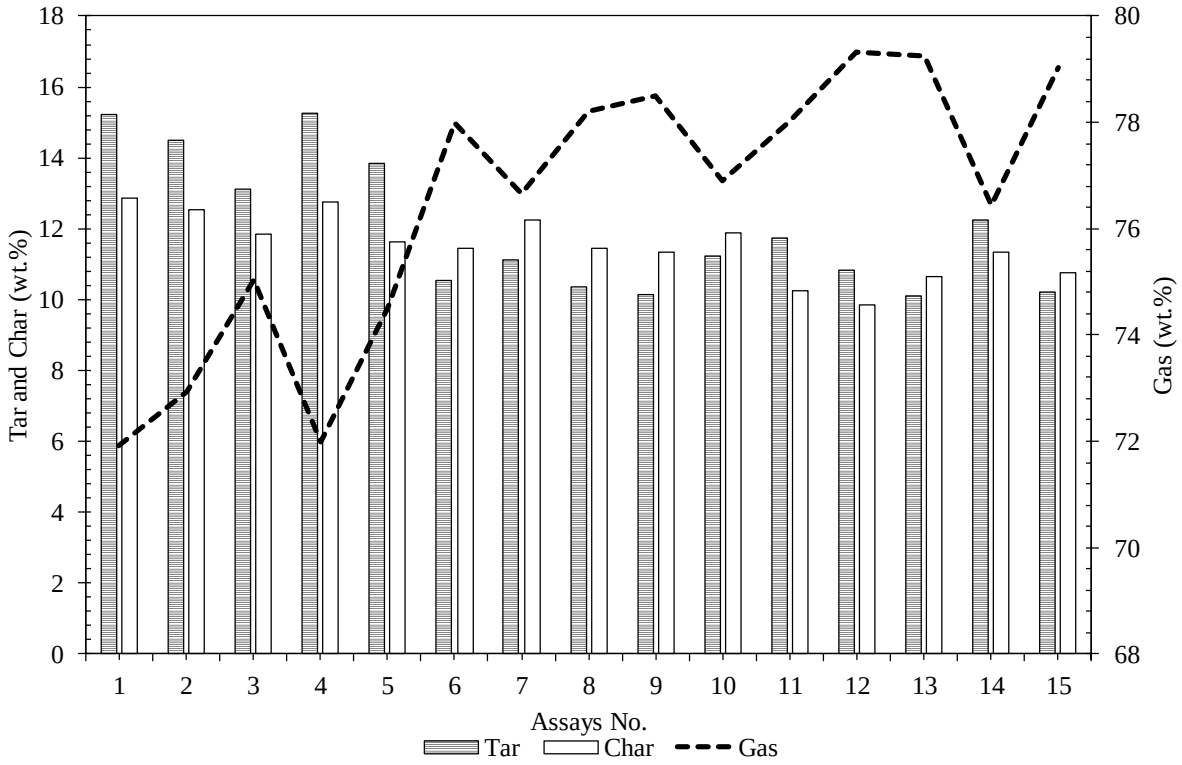

Fig. 2. Product distribution of SB biomass gasification under three different experimental conditions, temperature (700 – 900 ℃), SB loading (2 – 4 g) and residence time (10 – 30 min).

By varying the reactor temperature from 700 to 900 ºC, the gas yield increased considerably from 71.91 to 79.33 wt.%, whilst the bio-tar decreased sharply from 15.23 to 10.1 wt.%. In case of char, although it was decreased with increase in reactor temperature and residence time but not as bio-tar and is possibly converted into gas. The increment in gaseous yield could be ascribed to the conversion of bio-tar/vapors and char with respect to growing heating carrier temperature, subsequently higher bio-tar and char can be possibly altered into gas via thermal cracking reaction and Boudouard reaction, respectively [42]. The higher amounts of bio-tar and

char production were mainly supported by SB loading at lower temperature and residence time (Fig. 3 e and f). Yahaya et al. conducted the gasification two biomasses (coconut and palm kernel shell) and reported the thermal decomposition of tar and char with respect to increasing reactor temperature, leading to higher gas yield [43]. On the other hand, higher temperatures may facilitate the breakdown of C-C and C-O band, resulting in lower the particles size and encourage the probability of transforming them into reduced gas particles [25]. In general, bio-tar and char conversion into gaseous product is an endothermic process supported by tar cracking and Boudourad reactions [43]. Thus, an enhanced reactor temperature would thermodynamically favor the tar and char conversion into gas, thereby decrease the fractions of bio-tar and char in product distribution. These findings are similar with other studies reported [42, 44]. Luo et al. presented a novel concept to investigate the reliability of heat recovery from blast furnace (BF) slag as thermal media for gasification using a continuous moving-bed reactor. The results show that the increasing temperature from 800 – 1200 ℃ significantly enhanced the total gas yield, whilst tar and char were decreased. This phenomenon was attributed to the decomposition of tar and char via Boudourad and thermal cracking reactions at higher temperature [42]. Hu et al. explored the effect of reactor temperature on tar reduction from co-gasification of wet sewage and sawdust in a bench scale reactor. The results showed that the reactor temperature ranging from 600 to 900 ℃ not only considerably increased the gas yield from 63.43 wt.% to 80.58 wt.% but diminished tar (i.e. 15.34 to 2.19 wt.%) and char (i.e. 21.23 to 17.23 wt.%) yields [44]. The pyrolysis at low temperature (300 ℃) transforms up to 90 wt. % of the original organic solids to char due to high vapour residence time [45]. The bio-oil yields increases causing to a decline in char at moderate temperature (500 ℃). Beyond 500 ℃, the bio-oil declines with upsurge in temperature due to the thermal cracking (i.e., secondary tar reaction of the volatiles) [46],

resulting to increase in gas yield [47]. Thus, depending on the various parameters such as biomass composition, biomass particle size, heating rate and reactor temperature as well as the residence time, bio-tar and char could be altered into gaseous products comprising of H_2, CO, CO_2 and CH_4 [25]. Table 3 shows the analysis of variance (ANOVA) to construct the empirical prediction models and the significance of experimental parameters on gas, tar and char. Both linear and square effects with respect to experimental parameters were studied, including their interactions, on the product distribution. Typically, a mathematical model is considered as suitable when its ANOVA attains high statistical significance, with P-values <0.05, which shows a 95% confidence level. In addition, the P-value verifies the comparative rank of specific parameters. The smaller the P-value for a parameter, the more significant the parameter. For instance, for reaction products, the P-value (0.000) of reactor temperature was smaller than those of residence time (0.008), whereas SB loading had P-value of 0.392 (non-significant). This implies that the reactor temperature exhibited more contribution to the fitted model than residence time. The coefficient (R^2) and adjusted coefficient (R^2) corresponding to the gas, tar and char were found to be R^2 = 0.98, 0.99 and 0.97 and 0.97, 0.97 and 0.92, respectively.

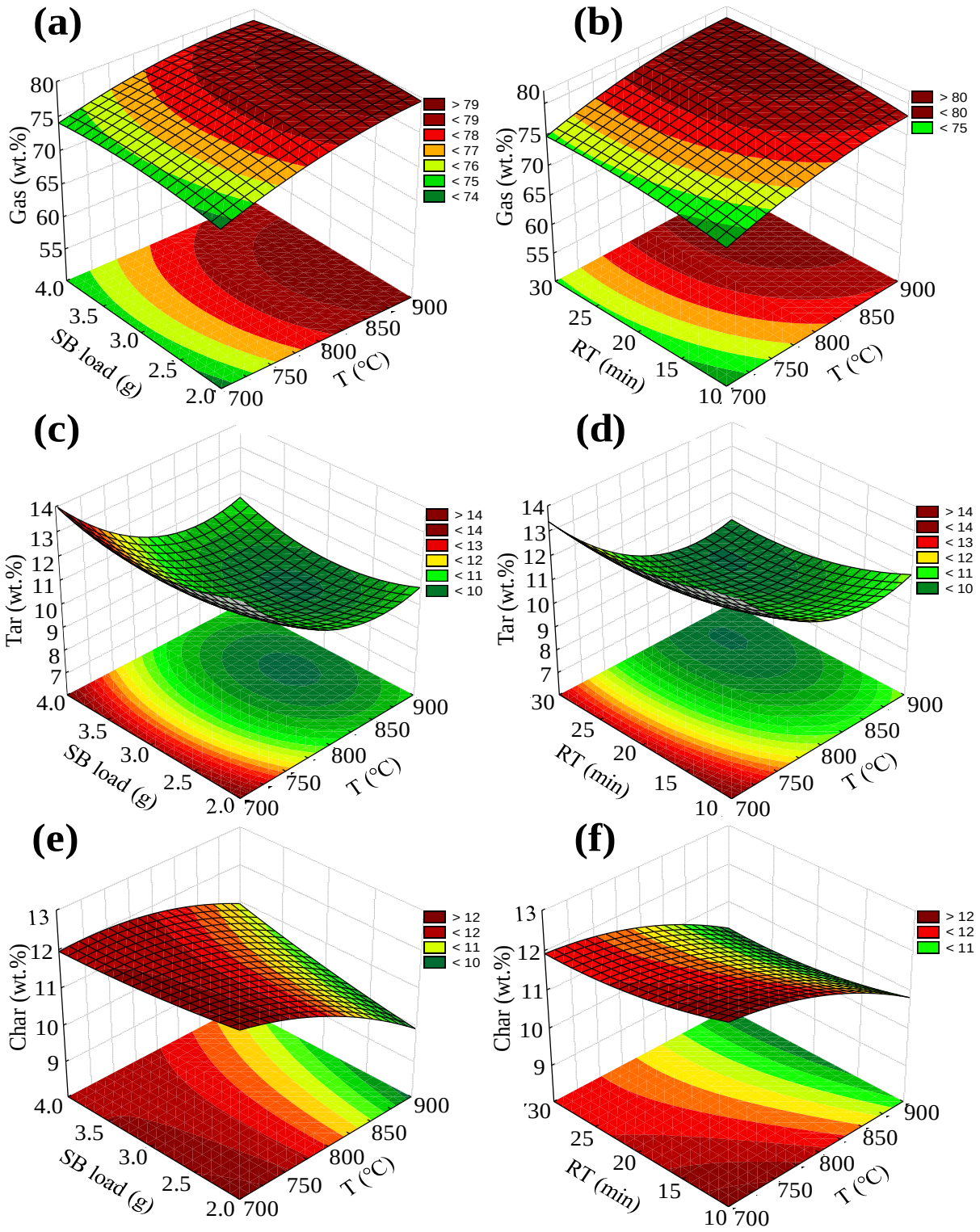

Fig. 3. Three-dimensional response plots (a-f) of gas, bio-tar and char: combined effect of temperature (700 – 900 ℃), SB loading (2 – 4 g) and residence time (10 – 30 min).

Table 3. ANOVA results for product distribution (Gas, Tar and Char).

	Gas (wt. %)			Tar (wt. %)			Char (wt. %)		
Response variables	SS	DF	P	SS	DF	P	SS	DF	P
Linear									
T*	65.99	1	<0.001	28.32	1	<0.001	7.84	1	<0.001
SB**	0.17	1	0.392	0.00	1	0.94	0.19	1	0.138
RT***	8.63	1	<0.001	3.63	1	<0.001	1.06	1	<0.008
Square									
T^2	3.49	1	<0.008	5.81	1	<0.001	0.29	1	0.079
SB^2	1.92	1	<0.025	1.58	1	<0.010	0.16	1	0.621
RT^2	1.38	1	<0.044	0.73	1	<0.041	0.10	1	0.249
Combined interaction									
T × SB	1.55	1	<0.037	0.03	1	0.584	1.13	1	<0.007
T × RT	0.01	1	0.791	0.08	1	0.399	0.02	1	0.531
SB × RT	0.94	1	0.079	0.38	1	0.104	0.12	1	0.216
Error / Lack of fit	0.98	5		0.49	5		0.30	5	
Total	93.78	14		49.89	14		11.02	14	
R^2	0.98			0.99			0.97		
Adj-R^2	0.97			0.97			0.92		

*T = Temperature; **SB = Sugarcane bagasse loading; ***RT = Reaction time

3.2. Analysis of gaseous products

The gasification was performed under varying conditions of temperature, SB loading and residence time. Regarding the selection of the well-fit model, as listed in Table S1, the quadratic model was suggested amongst all models, i.e. linear, 2FI, quadratic, and cubic (presented by DX-10 software) due to the minimum sequential P-value, and almost higher integrated values for Adjusted R^2 and Predicted R^2. Table S2 and Table 4 presents the gas constituents, such as H_2 (includes actual, predicted and residual values), CO, CO_2 and CH_4 as well as their lower heating value (LHV). During the tests, the H_2 and CO_2 were seen to be the main gases produced from gasification of SB.

As shown in Table S2, for all responses (i.e., H_2, CO, CO_2, and CH_4) the amount of p-value less than 0.05 confirms that all models are significant. However, the value of some statistical terms, such as the difference of adjusted R^2 and predicted R^2 which should be <0.2, was not desirable to prove the suitability of the models based on the experimental data and predicted values. The list and values of unmodified models are reported in Table S2. As listed in Table S2, undesirable statistical values (defined in the following) might cause a large block influence or a probable issue with the model and/or data. The possible way that should be taken into account are model reduction by eliminating insignificant terms, response transformation, outliers, etc. Additionally, according to the fundamental of the design method, it is possible to remove insignificant terms (holding p-value > 0.05) to simplify the model, and consequently, improve the statistical terms representing the accuracy and reliability of the model to predict the behavior of the system and/or mechanism (DX-10 [48]. Fermoso et al. studied the combined effect of operating variables such as temperature (900 - 1000℃), steam (25 – 55 vol.%) and oxygen (5 – 15 vol.%) concentration via response surface methodology for H_2 rich gas production from coal in high pressure fixed bed gasifier. They

performed ANOVA to examine the significance of quadratic model to the experimental data. The model terms were assessed by means of the p-value at a 95% confidence level. The insignificant terms (p-value > 0.05) from the models were removed to improve the model fitting [31]. Therefore, in the current study the insignificant terms for all responses (i.e., H_2, CO, CO_2 and CH_4) were eliminated to enhance the statistical terms of developed models as detailed in Table 4.

1 **Table 4.** ANOVA results for gaseous products

Responses Gas production (mol%)	**Final equations in terms of coded factors**	**Significant model terms**	**F-value**	**P-value**	**R^2**	**Ajd R^2**	**Pred R^2**	**Adeq. Precision**	**Std. Dev.**	**Mean**	**C.V. %**
H_2	+43.18 +3.65 A +0.46 B +1.55 C +1.84 BC -5.26 A^2 -5.16 B^2	Quadratic model: A, BC, A^2, B^2	13.50	0.0008 (<0.08%)	0.91	0.84	0.71	11.65	2.33	36.23	6.43
CO	+19.73 -0.23 A +0.80 B +1.22 C +3.64 A^2 -1.13 B^2 -1.21 C^2	Quadratic model: B, C, A^2, B^2, C^2	18.89	0.0003 (<0.03%)	0.93	0.88	0.75	13.11	0.70	20.60	3.42
CO_2	+20.66 -2.69 A -0.88 B -2.71 C +1.44 A^2 +3.87 B^2 +2.14 C^2	Quadratic model: A, C, B^2	9.04	0.0033 (<0.33%)	0.87	0.78	0.51	9.81	2.23	25.62	8.72
CH_4	+15.95 -0.73 A -0.38 B -0.06 C -1.34 BC +2.39 C^2	Quadratic model: BC, C^2	5.31	0.0152 (1.52%)	0.75	0.61	0.34	7.07	1.23	17.54	7.03

2

3

4

To be specific, an F-test is a statistical test that is often used to compare statistical correlations fitted to a set of data, in order to determine whether the correlation fits the data collection [49]. Briefly, the F-value of > 0.90 indicates that model is significant, and the desirable percentage of the P-value < 0.05% reveals only 0.05% probability for an F-value with that amount to occur because of noise (DX-10 [48]). For example, in the case of H_2 model shown in Table 4, F-value of 13.50 and desirable P-value percentage of <0.08% show the significance of quadratic model. In this work, due to the reliability and stability of machine and accuracy of results, the experiments were not repeated in the center point for several times, else another statistical term named Lack of Fit could be another good reference to show if a model fits the data or not [50].

The comparison of predicted R^2 and adjusted R^2 reveals the degree of the reasonable agreement between them. In the case of all developed models, the elimination of insignificant terms improved the statistical values, so that the predicted R^2 corresponding to all responses is in reasonable agreement with the adjusted R^2 with a difference less than 0.20, except CH_4. From the ANOVA analysis, the determination coefficient (R^2) and the adjusted determination (Adj. R^2) values for response variables (H_2, CO, CO_2 and CH_4) are sufficiently high, so that the suitability among the experimental and the predicted results are confirmed by desirable difference of adjusted R^2 and predicted R^2 (<0.2). Moreover, adequate precision is another measurement to depict the signal-to-noise ratio, which compares the range of predicted values at various operating conditions (the design points) to the average prediction error (DX-10 [48]). In fact, the adequate precision provides another way to evaluate the adequacy of a model for predictive purposes. The desirable ratio of aadequate precision is >4 which indicate adequate model discrimination [51]. According to the values listed in the Table 4, all developed models have adequate precision values >7 confirming their desirable amount. Furthermore, the coefficient of variance (C.V.%) is another term that is the ratio of estimated

standard error to the mean value of the response. In fact, C.V. < 10% indicates the high accuracy, reproducibility and dependability of the experiments [50-52]. According to the C.V. values presented in Table 4, all models possess a C.V. < 9.0% showing the great precision, reliability and dependability of the experimental data acquired and associated models for four above-mentioned responses. Nevertheless, in Table 4, the final equations are presented in coded factors, which can be applied to predict the effectiveness for specific level of each factor based on the coded amounts. The factors coded with +1 represent high level and factors coded with -1 are considered as the low level. The coded factors enable to identify the comparative influence of the any specific factor on response variable and its interactions by comparing the factors coefficients (DX-10 [48]). The ranges of the gas products composition were 25.12 – 42.88 mol% for H_2, 16.37 – 23.83 mol% for CO, 19.13 – 34.97 mol% for CO_2 and 14.12 – 20.86 mol% for CH_4. According to Table 2, the H_2 fraction of 42.88 mol% (36.91 g kg-biomass^{-1}) was obtained when experiment was conducted at 900 ℃ with 3 g of SB loading for 20 min of residence time. The lower H_2 of 25.12 mol% (14.64 g kg-biomass^{-1}) was attained at lower temperature (700 ℃), higher SB loading (4 g) and lower residence time (10 min). Similar results were found from other studies [5]. According to Fig. 2 (a, b) pertaining to H_2 production, a slightly higher H_2 can be also produced under other operating conditions with lower temperature (~800 ℃), equal SB amount (~3 gr), but higher retention time (~30 min). The exact optimum point in terms of highest H_2 production can be calculated by developed model for H_2 generation (shown in Table 4), in order to be nominated as the optimum experimental point in terms of lower energy consumption while higher energy generation. Nonetheless, the syngas LHV varied from 11.75 – 13.41 MJ Nm^{-3}. The syngas LHV of 14.92 MJ Nm^{-3} has been regarded appropriate for dissimilar industrial usages for instance gas engines, boilers and methanol [37].

The combined effect and variations of experimental parameters on syn-gas and by-products are shown in Fig. 4. The three-dimensional (3D) surface responses in Fig. 4 (a-h) display the H_2, CO, CO_2 and CH_4 production. According to Fig. 4 a and b, it can be observed that increasing reactor temperature and residence time are highly favorable experimental parameters to support the continuous H_2 production followed by SB loading. In Fig. 4 c and d, CO yields were also considerably supported by increasing reactor temperature, whereas increasing residence time and SB loading do not favor CO production. On the other hand, the increase in reactor temperature and residence time significantly decreased the CO_2 and CH_4 production (Fig. 4 f and h). This considerable increase in H_2 and CO production indicates temperature as the most important parameter during the biomass gasification. According to the Le Chatelier principles, higher reaction temperatures support reactants in endothermic reactions [5]. Therefore, endothermic reactions for instance waster-gas reaction ($C + H_2O \leftrightarrow CO + H_2$) [53, 54], reverse Boudoard reaction [$C\ (char) + CO_2 \leftrightarrow 2CO$)] [55] and reforming reaction ($CH_4 + CO_2 \leftrightarrow 2CO + 2H_2$) [56, 57] are the key dynamics behind the upsurge of H_2 and CO production and the decline of CO_2 and CH_4. Also, secondary reactions, for instance tar cracking and reforming may also promoted to an upsurge in H_2 and CO production [43].Thus, the simultaneous reactions and tar conversion (see Table 2 and Fig. 4 c and d) are the responsible for the upsurge of H_2 at higher temperature, lower SB loading and higher residence time. Furthermore, positive effect of residence time on H_2 production can be attributed to the heat transfer phenomenon, where longer residence time led to higher thermal decomposition of biomass into gas. Fermoso et al. gasified coal in fixed bed gasifier and reported significant increase in H_2 production via endothermic gasification reactions supported by increasing reaction temperature [31]. In addition, the heavy hydrocarbons at elevated temperatures favor H_2 production via the carbonization reaction ($C_nH_m \rightarrow {}_nC + m/2H_2$), thereby decreasing the tar content with increasing temperature [56]. Cao et al.

reported the decreasing trend of H_2 production with increase in SB biomass from 3 to 12 wt.%, while the molar fractions of CH_4 and CO_2 exhibited an escalating trend [5, 58]. However, in this study, compared to reactor temperature and residence time, SB showed negligible positive effect on H_2 production, which could be because of more reactive groups per unit volume to change the equilibrium of the water-gas shift reaction ($CO + H_2O \leftrightarrow CO_2 + H_2$) to the right [58, 59]. This could also be the reason of decreasing H_2 production that increasing SB loading would decrease the moisture content (moisture contained in biomass) in the reactor which in turn would suppress the steam reforming reaction ($CH_4 + H_2O \leftrightarrow CO + 3H_2$). Furthermore, increased biomass loading may cause less contact time per volume of oxidizing agent and thereby fewer oxygen interaction with feedstock [60]. Therefore, biomass loading increment caused less volatiles and consequently reduced the gasification process. As a result, the SB biomass sample remained partly gasified as reported in Fig. 2.

As shown in Fig. 4 e and f, an increase in temperature significantly decreases the fraction of CO_2 likely due to occurrence of the endothermic nature of the reactions such as Boudourad ($C + CO_2 \leftrightarrow 2CO$) and reverse water gas reaction ($CO_2 + H_2 \leftrightarrow CO + H_2O$) those are favored at high temperature, whereas steam methane reforming reactions ($CH_4 + H_2O \leftrightarrow CO + 3H_2$) decreased CH_4 fraction (Fig. 4 g and h). However, overall, more fraction of CO_2 than CO was observed in this study, where the ratio of CO/CO_2 ranged between 0.57 (see Table 2, run = 4 and 1.2 (see Table 2, run = 15).

Another noteworthy phenomenon could be that the WGS reaction ($CO + H_2O \leftrightarrow CO_2 + H_2$) performs a crucial role during biomass gasification to promote the H_2 fraction in gaseous products, where CO in the presence of moisture (contained in cellular structure of biomass) will be converted into H_2 and CO_2. As a results, CO fraction in current study was reduced as

shown in Table 2 and Fig. 4 c and d. Cao et al. and others reported the similar trend, indicating that the promotion of H_2 and CO fractions regarding reactor temperature was eased through endothermic nature of the primary gasification and the secondary reactions [5, 61]. On the whole, a higher temperature, a lower SB loading and a longer residence time supported the gasification of SB, leading to a higher H_2 production in gaseous products.

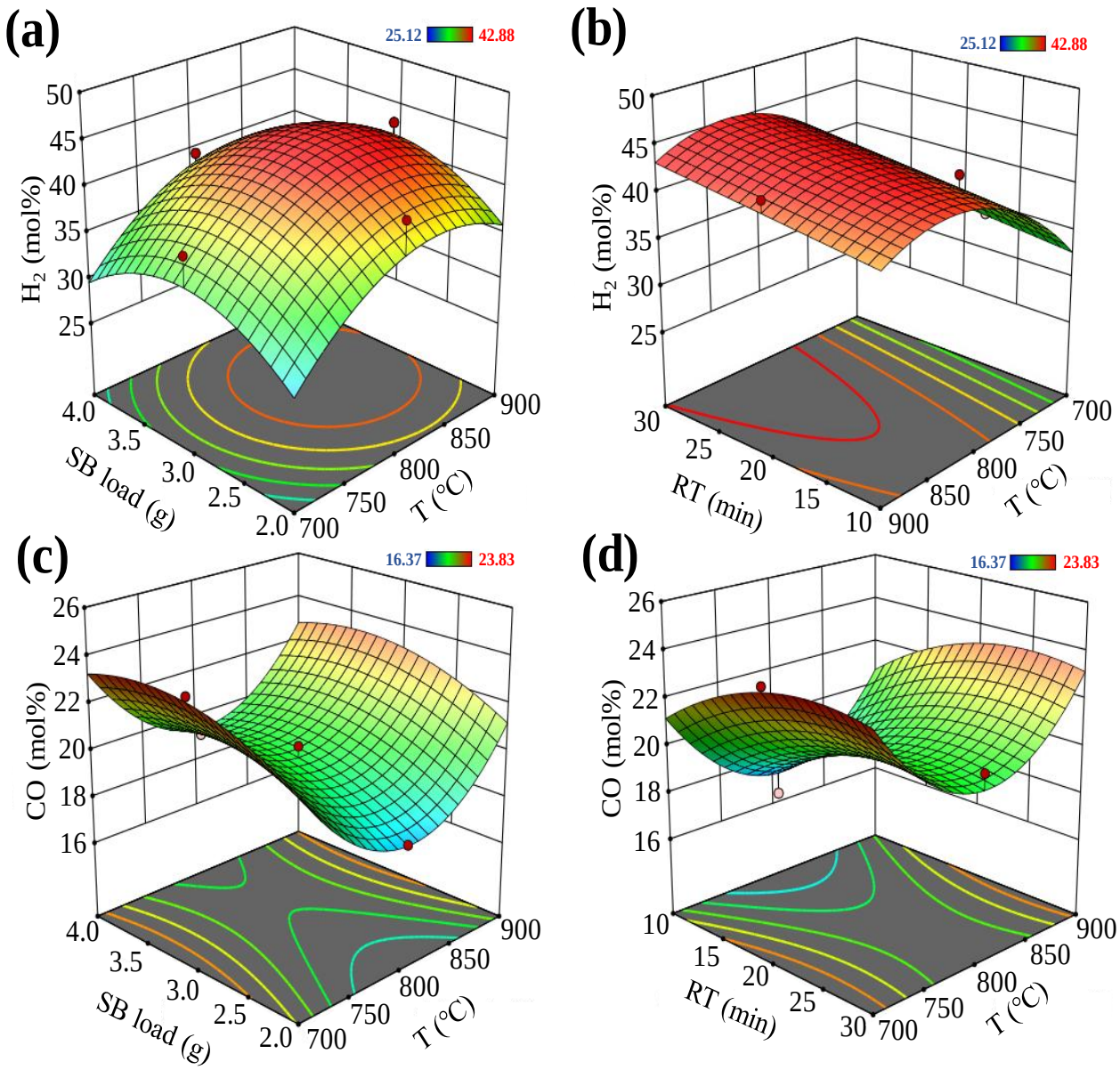
(a)
25.12
42.88
H2 (mol%)
50
45
40
35
30
25
4.0
3.5
3.0
2.5
2.0
SB load (g)
700
750
800
850
900
T (°C)
(b)
25.12
42.88
H2 (mol%)
50
45
40
35
30
25
30
25
20
15
10
RT (min)
700
750
800
850
900
T (°C)
(c)
16.37
23.83
CO (mol%)
26
24
22
20
18
16
4.0
3.5
3.0
2.5
2.0
SB load (g)
700
750
800
850
900
T (°C)
(d)
16.37
23.83
CO (mol%)
26
24
22
20
18
16
10
15
20
25
30
RT (min)
700
750
800
850
900
T (°C)

1

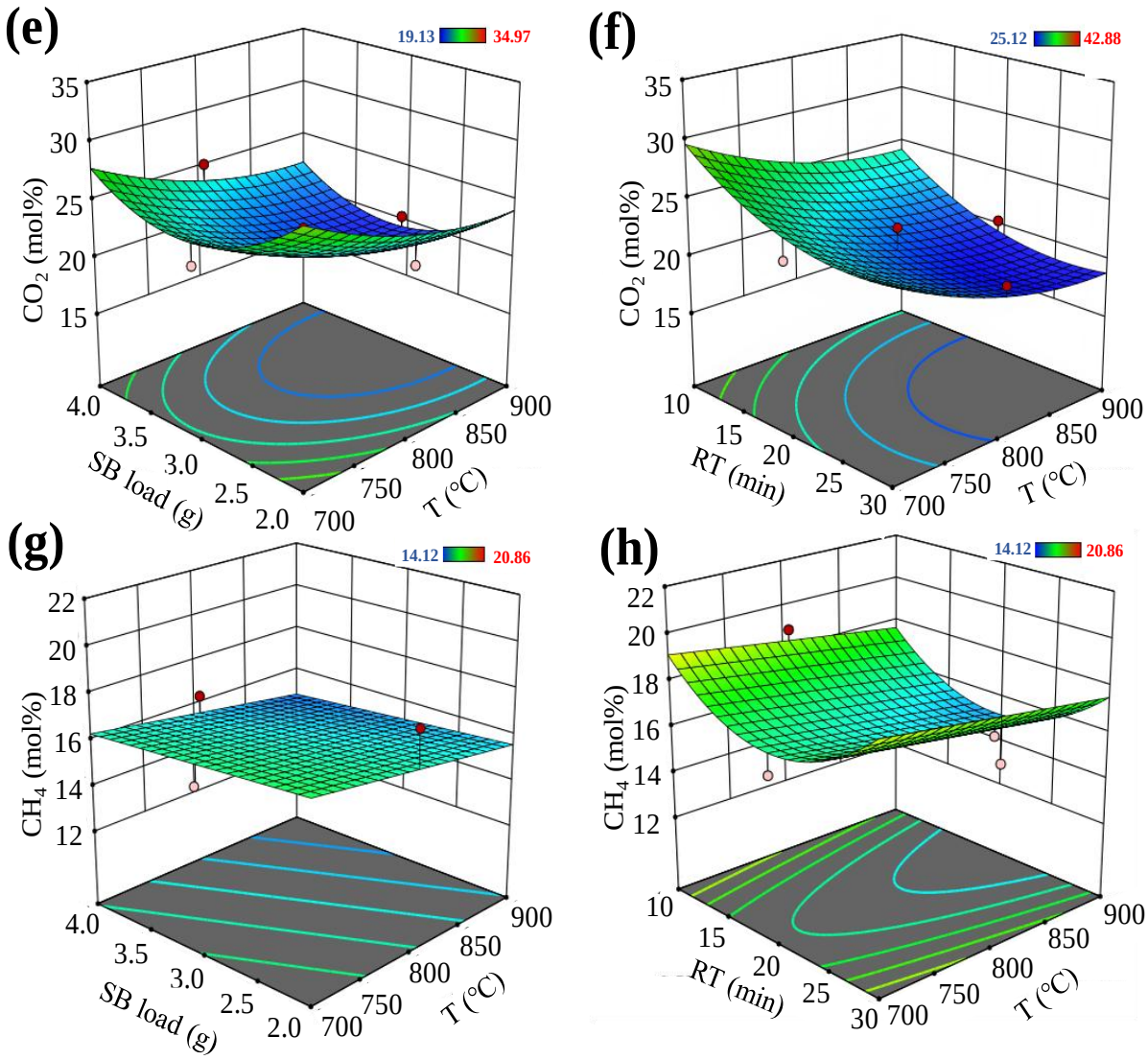

Fig. 4. Three-dimensional response plots (a-h) of H_2, CO, CO_2 and CH_4 production: combined effect of temperature (700 – 900 ℃), SB loading (2 – 4 g) and residence time (10 – 30 min).

3.3. Statistical optimization of gaseous product

The results from the CCD were tested via statistical analysis to ascertain the significant process parameters that influence the production of gas constituents. According to analysis, the H_2 production estimation can be achieved via a quadratic regression model:

H_2 concentration

$$= 3.65\, x_1 - 5.65\, x_1^2 - 5.16\, x_2^2 + 1.84\, x_2\, x_3 + 1.55\, x_3 + 0.4560\, x_2$$

Where x_1, x_2 and x_3 indicate the reactor temperature, SB loading and residence time. The standardized Pareto chart in Fig. 5, shows the simplified influence of each experimental parameters on H_2 production. As mentioned, Design Expert (DX v. 10) was used to accomplish the analysis of variance (ANOVA) and the corresponding effects are given in Table 4. ANOVA analysis confirms the statistical importance of the variables and appropriateness of the model. The values of $p<0.05$ specify that the model parameters are significant. Thus, amongst the three experimental parameters, temperature (T) was observed as the most significant parameter with p-value of <0.0011. This is followed by residence time, which has supported H_2 production with p-value of 0.0689. However, SB loading did not support H_2 production. Cao et al. and Rashidi et al. reported temperature as the most significant experimental parameter when gasifying SB followed by residence time, whereas increasing SB loading decreased H_2 concentration in gaseous products [5, 62]. This infers that the reaction temperature and residence time are the most crucial parameters that support the total gas and H_2 yield in SB gasification. Furthermore, considerably square and interaction/combined model terms for syngas (H_2 and CO) production are: T^2, SB^2, SB × RT and T^2, SB^2, RT^2 with p-value of 0.0054, 0.0060, 0.0562 and <0.0001, 0.0333, and 0.0251, respectively.

The effectiveness of the selected model was further validated based on the correlation co-efficient value. From the ANOVA analysis, the very high amount for determination coefficient (R^2) and the adjusted determination (Adj. R^2) values for response variables (H_2, CO, CO_2 and CH_4) are sufficiently high, so that the suitability among the experimental and the predicted results are confirmed by desirable difference of adjusted R^2 and predicted R^2

(<0.2). Moreover, it also indicates that the experimental results and the predicted values are in good agreement as shown in Table 2.

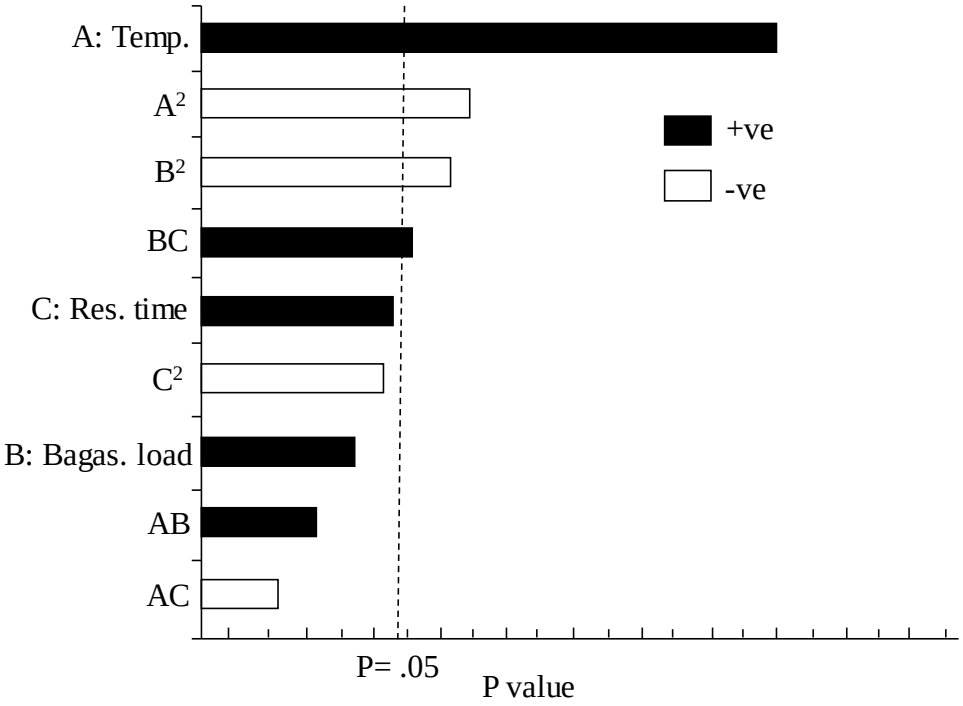

Fig. 5. Standardized Pareto char for H_2 production from SB biomass gasification. Amongst the parameters studied, temperature is the highly significant parameter to support H_2 production in product gas. +ve signs shows synergistic effect and –ve sign shows antagonistic effect of specific parameters on desired product.

3.4 Diagnostics of Response Models

The validation of developed models for the production of H_2, CO, CO_2, and CH_4 can be verified considering few diagnostic plots, namely normal probability vs residual plot, residual vs experimental data plot and residual vs predicted plot. Generally, aforementioned plots are used in order to confirm the residual analysis of the RSM-CCD and to certify the analysis data fit with the aid of statistical assumptions. To be specific, normal probability plot helps to determine whether the experimental results follow a normal distribution [51]. Regarding normal probability vs. residual plot, the model normalcy assumption is regarded

as satisfied if the residual plot stays on a straight line [52, 63]. Various major plots have been shown in Fig. 6, Fig. 7 and Fig. S1, consequently. As shown in Fig. 6, all the points are lying very near to the straight line of 45-degree without any kurtosis or skewness in the sample distribution, indicating that the normal distribution of the standard deviations between the actual and the predicted values [64, 65].

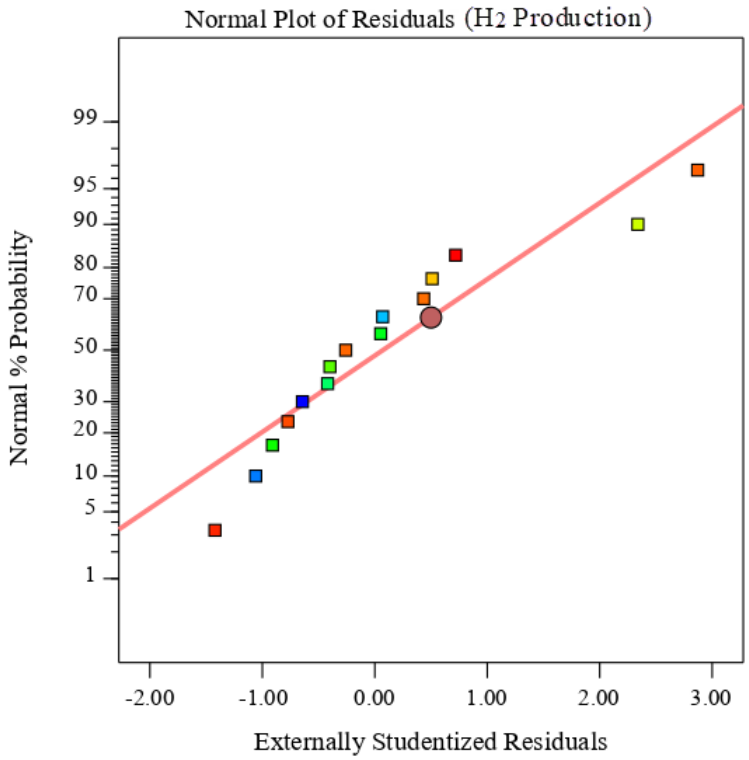

Fig. 6. Normal probability vs. residuals for H_2 production.

Additionally, the plots (i.e., externally standardized residuals) considered for representing residuals vs. experimental data and residuals vs. predicted are capable and accessible approaches in order to identify the outlier results for each actual data and predicted values, respectively [51, 66].

In terms of residual vs. predicted plot of responses, the suggested models maybe used, when most of points corresponding to empirical data are arbitrarily distributed in constant range of residuals across the plot (i.e., surrounded by the horizontal lines possessing a spectrum of

±delta [67]. Thus, as elucidated in Fig. 7 (a and b), the discrepancies within results and potentially influencing outliers were identified neither for the empirical data nor predicted values.

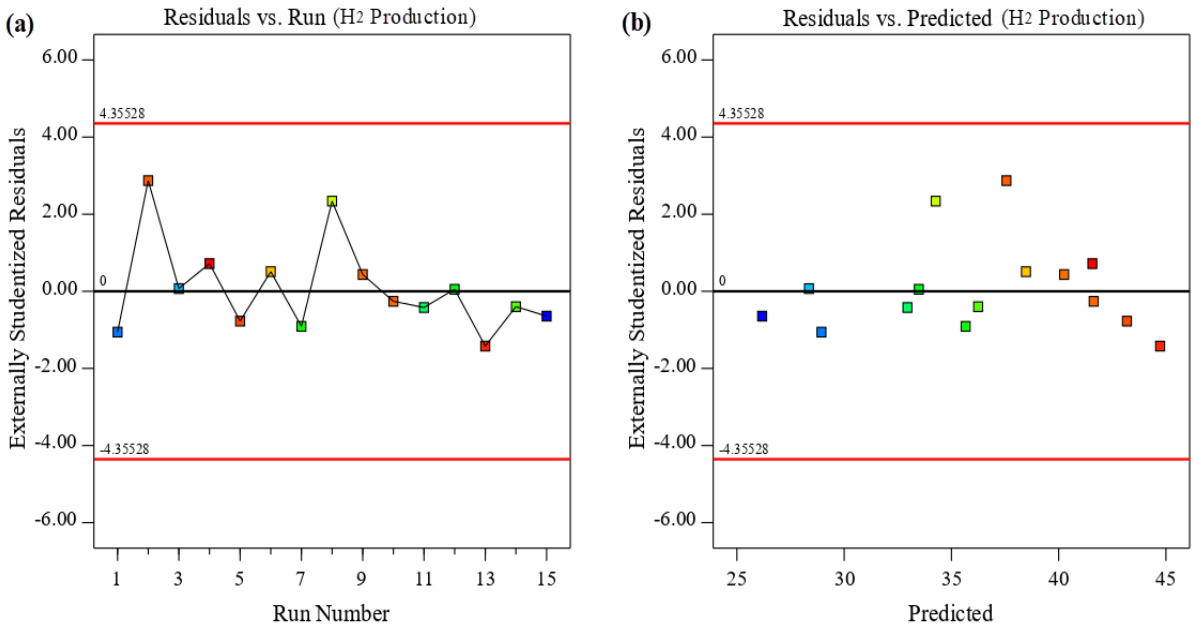

Fig. 7. The plots of (a) residuals vs. experiments and (b) residuals vs. predicted values for H_2 production.

Fig. S1 Shows the models authentication by removing (a) CO, (b) CO_2 and (c) CH_4 production with the help of normal probability vs. residual, residual vs. run and residual vs. predicted plots. As depicted in **Fig. S1**, most of the respective points are near the straight line of 45-degree without any kurtosis or skewness in the sample distribution, indicating the normal distribution of empirical data. Furthermore, the plots of superficially standardized residuals exercised for showing residuals vs. experimental and residuals vs. predicted are effective and obtainable approaches to identify the outlier data for each actual experimental data and predicted values, respectively. So, as demonstrated in Fig. SI (a - c), the contradictories result and influencing outliers were identified neither for the empirical data nor predicted values.

4. Conclusion

The gasification of SB biomass was performed using central composite design. The statistical analysis conducted in order to study the effect of experimental parameters on responses (H_2, CO, CO_2, and CH_4). The development of interaction amongst the experimental parameters stipulated constructive statistics in relation to the SB gasification process that would not have been known, by means of the conventional manual experimental methods. Based on the response plots referring to the models and the ANOVA results, reactor temperature was the most influential parameter followed by residence time. An upsurge in the reactor temperature and influential considerably decreased the production of bio-tar, CO_2 and CH_4 fractions. Optimum conditions to obtained highest yield of H_2 include a temperature of 900 ºC, the SB loading of 3 g and the residence time of 20 min. Overall, it was incurred that an elevated reaction temperature, a lower SB loading and extended reaction time support the gasification of SB, leading to a hydrogen-rich gas production.

Acknowledgement

The work was supported by National Natural Science Foundation of China (grant number: 51506112), Tsinghua University Initiative Scientific Research Program (grant number: 20161080094). EPSRC grant EP/G01244X/1 (Supergen Consortium XIV Sustainable Delivery of Hydrogen).

References

[1] Ahmed I, Gupta A. Sugarcane bagasse gasification: global reaction mechanism of syngas evolution. Applied Energy. 2012;91:75-81.

[2] Yang Q, Zhou H, Zhang X, Nielsen CP, Li J, Lu X, et al. Hybrid life-cycle assessment for energy consumption and greenhouse gas emissions of a typical biomass gasification power plant in China. Journal of Cleaner Production. 2018;205:661-71.

[3] Cherubini F, Bird ND, Cowie A, Jungmeier G, Schlamadinger B, Woess-Gallasch S. Energy-and greenhouse gas-based LCA of biofuel and bioenergy systems: Key issues, ranges and recommendations. Resources, conservation and recycling. 2009;53:434-47.

[4] Bundhoo ZM. Potential of bio-hydrogen production from dark fermentation of crop residues: A review. International Journal of Hydrogen Energy. 2018.

[5] Cao W, Guo L, Yan X, Zhang D, Yao X. Assessment of sugarcane bagasse gasification in supercritical water for hydrogen production. International Journal of Hydrogen Energy. 2018.

[6] Shukla A, Kumar SY. A Comparative study of Sugarcane Bagasse gasification and Direct Combustion. International Journal of Applied Engineering Research. 2017;12:14739-45.

[7] Bezerra TL, Ragauskas AJ. A review of sugarcane bagasse for second-generation bioethanol and biopower production. Biofuels, Bioproducts and Biorefining. 2016;10:634-47.

[8] Asadullah M. Barriers of commercial power generation using biomass gasification gas: a review. Renewable and Sustainable Energy Reviews. 2014;29:201-15.

[9] Klein BC, Chagas MF, Junqueira TL, Rezende MCAF, de Fátima Cardoso T, Cavalett O, et al. Techno-economic and environmental assessment of renewable jet fuel production in integrated Brazilian sugarcane biorefineries. Applied Energy. 2018;209:290-305.

[10] Hu B-B, Li M-Y, Wang Y-T, Zhu M-J. High-yield biohydrogen production from non-detoxified sugarcane bagasse: Fermentation strategy and mechanism. Chemical Engineering Journal. 2018;335:979-87.

[11] Martínez O, Sánchez A, Font X, Barrena R. Enhancing the bioproduction of value-added aroma compounds via solid-state fermentation of sugarcane bagasse and sugar beet molasses: Operational strategies and scaling-up of the process. Bioresource technology. 2018;263:136-44.

[12] Martínez O, Sánchez A, Font X, Barrena R. Valorization of sugarcane bagasse and sugar beet molasses using Kluyveromyces marxianus for producing value-added aroma compounds via solid-state fermentation. Journal of Cleaner Production. 2017;158:8-17.

[13] Thungklin P, Sittijunda S, Reungsang A. Sequential fermentation of hydrogen and methane from steam-exploded sugarcane bagasse hydrolysate. International Journal of Hydrogen Energy. 2018.

[14] Mustafa AM, Li H, Radwan AA, Sheng K, Chen X. Effect of hydrothermal and Ca (OH) 2 pretreatments on anaerobic digestion of sugarcane bagasse for biogas production. Bioresource technology. 2018;259:54-60.

[15] Lima DRS, Adarme OFH, Baêta BEL, Gurgel LVA, de Aquino SF. Influence of different thermal pretreatments and inoculum selection on the biomethanation of sugarcane bagasse by solid-state anaerobic digestion: A kinetic analysis. Industrial Crops and Products. 2018;111:684-93.

[16] Ribeiro FR, Passos F, Gurgel LVA, Baêta BEL, de Aquino SF. Anaerobic digestion of hemicellulose hydrolysate produced after hydrothermal pretreatment of sugarcane bagasse in UASB reactor. Science of the Total Environment. 2017;584:1108-13.

[17] Xie W, Wen S, Liu J, Xie W, Kuo J, Lu X, et al. Comparative thermogravimetric analyses of co-combustion of textile dyeing sludge and sugarcane bagasse in carbon

dioxide/oxygen and nitrogen/oxygen atmospheres: Thermal conversion characteristics, kinetics, and thermodynamics. Bioresource technology. 2018;255:88-95.
[18] Galina NR, Luna CMR, Arce GL, Ávila I. Comparative study on combustion and oxy-fuel combustion environments using mixtures of coal with sugarcane bagasse and biomass sorghum bagasse by the thermogravimetric analysis. Journal of the Energy Institute. 2018.
[19] Centeno-González FO, Lora EES, Nova HFV, Neto LJM, Reyes AMM, Ratner A, et al. CFD modeling of combustion of sugarcane bagasse in an industrial boiler. Fuel. 2017;193:31-8.
[20] Ghorbannezhad P, Firouzabadi MD, Ghasemian A, de Wild PJ, Heeres H. Sugarcane bagasse ex-situ catalytic fast pyrolysis for the production of Benzene, Toluene and Xylenes (BTX). Journal of Analytical and Applied Pyrolysis. 2018;131:1-8.
[21] David GF, Justo OR, Perez VH, Garcia-Perez M. Thermochemical conversion of sugarcane bagasse by fast pyrolysis: High yield of levoglucosan production. Journal of Analytical and Applied Pyrolysis. 2018.
[22] Varma AK, Mondal P. Pyrolysis of sugarcane bagasse in semi batch reactor: effects of process parameters on product yields and characterization of products. Industrial crops and products. 2017;95:704-17.
[23] Sahoo A, Ram DK. Gasifier performance and energy analysis for fluidized bed gasification of sugarcane bagasse. Energy. 2015;90:1420-5.
[24] Sheikhdavoodi MJ, Almassi M, Ebrahimi-Nik M, Kruse A, Bahrami H. Gasification of sugarcane bagasse in supercritical water; evaluation of alkali catalysts for maximum hydrogen production. Journal of the Energy Institute. 2015;88:450-8.
[25] Anukam A, Mamphweli S, Reddy P, Meyer E, Okoh O. Pre-processing of sugarcane bagasse for gasification in a downdraft biomass gasifier system: A comprehensive review. Renewable and Sustainable Energy Reviews. 2016;66:775-801.
[26] Salam MA, Ahmed K, Akter N, Hossain T, Abdullah B. A review of hydrogen production via biomass gasification and its prospect in Bangladesh. International Journal of Hydrogen Energy. 2018;43:14944-73.
[27] Aydin ES, Yucel O, Sadikoglu H. Experimental study on hydrogen-rich syngas production via gasification of pine cone particles and wood pellets in a fixed bed downdraft gasifier. International Journal of Hydrogen Energy. 2019.
[28] Tavasoli A, Barati M, Karimi A. Sugarcane bagasse supercritical water gasification in presence of potassium promoted copper nano-catalysts supported on γ-Al2O3. International Journal of Hydrogen Energy. 2016;41:174-80.
[29] Barati M, Babatabar M, Tavasoli A, Dalai AK, Das U. Hydrogen production via supercritical water gasification of bagasse using unpromoted and zinc promoted Ru/γ-Al2O3 nanocatalysts. Fuel Processing Technology. 2014;123:140-8.
[30] Osada M, Yamaguchi A, Hiyoshi N, Sato O, Shirai M. Gasification of sugarcane bagasse over supported ruthenium catalysts in supercritical water. Energy & Fuels. 2012;26:3179-86.
[31] Fermoso J, Gil MV, Arias B, Plaza MG, Pevida C, Pis J, et al. Application of response surface methodology to assess the combined effect of operating variables on high-pressure coal gasification for H2-rich gas production. international journal of hydrogen energy. 2010;35:1191-204.
[32] Yusup S, Khan Z, Ahmad MM, Rashidi NA. Optimization of hydrogen production in in-situ catalytic adsorption (ICA) steam gasification based on Response Surface Methodology. biomass and bioenergy. 2014;60:98-107.
[33] Varma AK, Mondal P. Physicochemical characterization and pyrolysis kinetic study of sugarcane bagasse using thermogravimetric analysis. Journal of Energy Resources Technology. 2016;138:052205.

[34] Doumer ME, Arízaga GGC, da Silva DA, Yamamoto CI, Novotny EH, Santos JM, et al. Slow pyrolysis of different Brazilian waste biomasses as sources of soil conditioners and energy, and for environmental protection. Journal of Analytical and Applied Pyrolysis. 2015;113:434-43.
[35] Balasundram V, Ibrahim N, Kasmani RM, Isha R, Hamid MKA, Hasbullah H, et al. Catalytic upgrading of sugarcane bagasse pyrolysis vapours over rare earth metal (Ce) loaded HZSM-5: Effect of catalyst to biomass ratio on the organic compounds in pyrolysis oil. Applied Energy. 2018;220:787-99.
[36] Raheem A, Sivasangar S, Azlina WW, Yap YT, Danquah MK, Harun R. Thermogravimetric study of Chlorella vulgaris for syngas production. Algal research. 2015;12:52-9.
[37] Raheem A, Dupont V, Channa AQ, Zhao X, Vuppaladadiyam AK, Taufiq-Yap Y-H, et al. Parametric characterization of air gasification of Chlorella vulgaris biomass. Energy & Fuels. 2017;31:2959-69.
[38] Mohammed M, Salmiaton A, Azlina WW, Amran MM, Fakhru'l-Razi A. Air gasification of empty fruit bunch for hydrogen-rich gas production in a fluidized-bed reactor. Energy Conversion and Management. 2011;52:1555-61.
[39] Raheem A, Dupont V, Channa AQ, Zhao X, Vuppaladadiyam AK, Taufiq-Yap Y-H, et al. Parametric characterisation of air gasification of chlorella vulgaris biomass. Energy and Fuels. 2017;31: 2959–69.
[40] Chen J, Zhao K, Zhao Z, He F, Huang Z, Wei G. Identifying the roles of MFe2O4 (M= Cu, Ba, Ni, and Co) in the chemical looping reforming of char, pyrolysis gas and tar resulting from biomass pyrolysis. International Journal of Hydrogen Energy. 2019.
[41] Lv X, Xiao J, Shen L, Zhou Y. Experimental study on the optimization of parameters during biomass pyrolysis and char gasification for hydrogen-rich gas. International Journal of Hydrogen Energy. 2016;41:21913-25.
[42] Luo S, Zhou Y, Yi C. Hydrogen-rich gas production from biomass catalytic gasification using hot blast furnace slag as heat carrier and catalyst in moving-bed reactor. international journal of hydrogen energy. 2012;37:15081-5.
[43] Yahaya AZ, Somalu MR, Muchtar A, Sulaiman SA, Daud WRW. Effect of particle size and temperature on gasification performance of coconut and palm kernel shells in downdraft fixed-bed reactor. Energy. 2019;175:931-40.
[44] Hu M, Gao L, Chen Z, Ma C, Zhou Y, Chen J, et al. Syngas production by catalytic in-situ steam co-gasification of wet sewage sludge and pine sawdust. Energy Conversion and Management. 2016;111:409-16.
[45] Manara P, Zabaniotou A. Towards sewage sludge based biofuels via thermochemical conversion–a review. Renewable and Sustainable Energy Reviews. 2012;16:2566-82.
[46] Fonts I, Gea G, Azuara M, Ábrego J, Arauzo J. Sewage sludge pyrolysis for liquid production: a review. Renewable and sustainable energy reviews. 2012;16:2781-805.
[47] Park HJ, Heo HS, Park Y-K, Yim J-H, Jeon J-K, Park J, et al. Clean bio-oil production from fast pyrolysis of sewage sludge: effects of reaction conditions and metal oxide catalysts. Bioresource technology. 2010;101:S83-S5.
[48] Software D-E. State-Ease Inc. .
[49] Lomax R. Statistical Concepts: A Second Course (2007). ISBN 0–8058–5850–4; 2007.
[50] Dastyar W, Amani T, Elyasi S. Investigation of affecting parameters on treating high-strength compost leachate in a hybrid EGSB and fixed-bed reactor followed by electrocoagulation–flotation process. Process Safety and Environmental Protection. 2015;95:1-11.
[51] Ghaedi H, Ayoub M, Sufian S, Murshid G, Farrukh S, Shariff AM. Investigation of various process parameters on the solubility of carbon dioxide in phosphonium-based

deep eutectic solvents and their aqueous mixtures: Experimental and modeling. International Journal of Greenhouse Gas Control. 2017;66:147-58.
[52] Ishak S, Malakahmad A. Optimization of Fenton process for refinery wastewater biodegradability augmentation. Korean Journal of Chemical Engineering. 2013;30:1083-90.
[53] Ling M, Esfahani MJ, Akbari H, Foroughi A. Effects of residence time and heating rate on gasification of petroleum residue. Petroleum Science and Technology. 2016;34:1837-40.
[54] Vejahati F, Katalambula H, Gupta R. Entrained-flow gasification of oil sand coke with coal: assessment of operating variables and blending ratio via response surface methodology. Energy & Fuels. 2011;26:219-32.
[55] Raheem A, Dupont V, Channa AQ, Zhao X, Vuppaladadiyam AK, Taufiq-Yap Y-H, et al. Parametric characterisation of air gasification of chlorella vulgaris biomass. Energy & Fuels. 2017.
[56] Nam H, Maglinao AL, Capareda SC, Rodriguez-Alejandro DA. Enriched-air fluidized bed gasification using bench and pilot scale reactors of dairy manure with sand bedding based on response surface methods. Energy. 2016;95:187-99.
[57] Midilli A, Dogru M, Howarth CR, Ayhan T. Hydrogen production from hazelnut shell by applying air-blown downdraft gasification technique. International Journal of Hydrogen Energy. 2001;26:29-37.
[58] Samiee-Zafarghandi R, Karimi-Sabet J, Abdoli MA, Karbassi A. Supercritical water gasification of microalga Chlorella PTCC 6010 for hydrogen production: Box-Behnken optimization and evaluating catalytic effect of MnO2/SiO2 and NiO/SiO2. Renewable Energy. 2018;126:189-201.
[59] Raheem A, WAKG WA, Yap YT, Danquah MK, Harun R. Optimization of the microalgae Chlorella vulgaris for syngas production using central composite design. Rsc Advances. 2015;5:71805-15.
[60] Wan Ab Karim Ghani W, Moghadam RA, Salleh M, Alias AB. Air gasification of agricultural waste in a fluidized bed gasifier: hydrogen production performance. Energies. 2009;2:258-68.
[61] Chen J, Lu Y, Guo L, Zhang X, Xiao P. Hydrogen production by biomass gasification in supercritical water using concentrated solar energy: System development and proof of concept. International journal of hydrogen Energy. 2010;35:7134-41.
[62] Rashidi M, Tavasoli A. Hydrogen rich gas production via supercritical water gasification of sugarcane bagasse using unpromoted and copper promoted Ni/CNT nanocatalysts. The Journal of Supercritical Fluids. 2015;98:111-8.
[63] Elyasi S, Amani T, Dastyar W. A comprehensive evaluation of parameters affecting treating high-strength compost leachate in anaerobic baffled reactor followed by electrocoagulation-flotation process. Water, Air, & Soil Pollution. 2015;226:116.
[64] Shahrezaei F, Mansouri Y, Zinatizadeh AAL, Akhbari A. Process modeling and kinetic evaluation of petroleum refinery wastewater treatment in a photocatalytic reactor using TiO2 nanoparticles. Powder Technology. 2012;221:203-12.
[65] Amani T, Veysi K, Dastyar W, Elyasi S. Studying interactive effects of operational parameters on continuous bipolar electrocoagulation–flotation process for treatment of high-load compost leachate. International journal of environmental science and technology. 2015;12:2467-74.
[66] Montgomery DC. Design and analysis of experiments. seventh ed. New York: John Wiley & Sons, Inc.; 2008.
[67] Mansouri Y, Zinatizadeh AA, Mohammadi P, Irandoust M, Akhbari A, Davoodi R. Hydraulic characteristics analysis of an anaerobic rotatory biological contactor (AnRBC)

using tracer experiments and response surface methodology (RSM). Korean Journal of Chemical Engineering. 2012;29:891-902.